


CFD simulation of a shell and multiple tubes condensing heat exchanger in a modified microwave plant applied for reprocessing End of Life Tires (ELTs)

Roohollah Babaei-Mahani¹ | Pouyan Talebizadeh Sardari² | Salman Masoudi Soltani¹  | Hayder I. Mohammed³ | Zbigniew Kuncewicz⁴ | Christine Starr⁴

¹Department of Chemical Engineering, Brunel University London, Uxbridge, UB8 3PH, United Kingdom

²Centre for Sustainable Energy Use in Food Chains, Institute of Energy Futures, Brunel University London, Uxbridge, UB8 3PH, UK

³Department of Physics, College of Education, University of Garmian, Kalar, Iraq

⁴Tyre Recovered Commodities Ltd., Heywood, Lancashire, UK

Correspondence:

S. Masoudi Soltani Department of Chemical Engineering, Brunel University London, Uxbridge, UK
Email: Salman.MasoudiSoltani@brunel.ac.uk

Abstract

The condensation heat exchanger has a critical role in the microwave reduction process to separate and capture valuable by-products after the microwave reactor. This study aims to perform a computational fluid dynamics (CFD) simulation of a condenser to assess the heat transfer performance of the heat exchanger comprehensively. The type of heat exchanger used for this study is based upon an existing industrial-scale condenser taken from a conventional thermal pyrolysis end of tires (ELT) reprocessing plant and repurposed for integration into a 1500 kg/h ELT microwave reduction process. The condenser is a shell-and-multiple-tube heat exchanger in which the syngas passes through the tubes while cold water from a cooling tower is placed inside the shell. After the simulation, the effects of inlet temperatures and mass flow rates of the gas and water are investigated. The results show that the heat transfer rate is 58 kW for the inlet air velocity of 0.25 m/s and increases due to the convective heat transfer by 32% and 55% when the air velocity rises to 0.5 and 1 m/s, respectively, for the inlet gas and water temperatures of 80 and 15°C, respectively. Additionally, because the outlet air temperature and the inlet water temperature are strongly correlated with convective heat transfer, the outlet air temperature is equivalent to 17.2, 22.3, and 29.5°C when the inlet water temperature is 15, 20, and 25°C, respectively.

KEYWORDS

condenser, heat exchanger, microwave technology, reduction process, sensitivity analysis

1 | INTRODUCTION

Microwave processing utilizes electromagnetic waves of frequencies between 300 MHz and 300 GHz which generate heat in a material (Budarin et al., 2015; Thostenson & Chou, 1999; Zhou et al., 2022). The applications of microwave technology are vast, from small kitchen ovens to industrial processes (Das et al., 2009; Lam & Chase, 2012).

The microwave reduction process is relatively new. Conventional thermal heating usually employs an external heating source to transfer heat to material through a surface. In contrast, microwave heating constitutes a unique way of heating where the heating effect arises from the interaction of the electromagnetic wave with the dipoles within the material being heated (Lawag & Ali, 2022; Liu et al., 2019; Motasemi & Afzal, 2013). By such heating mechanisms, heat is generated within

This is an open access article under the terms of the [Creative Commons Attribution](https://creativecommons.org/licenses/by/4.0/) License, which permits use, distribution and reproduction in any medium, provided the original work is properly cited.

© 2023 The Authors. *Environmental Quality Management* published by Wiley Periodicals LLC.

the material rather than from an external source, thereby giving a more efficient heating process compared to conventional surface heating concerning even distribution of heat and easier control over the heating (Al Mamun et al., 2015; Metaxas, 1991). In addition, high temperatures and heating rates can be obtained through microwave heating (Ludlow-Palafox & Chase, 2001) demonstrating remarkably high conversion efficiency of electrical energy into heat (80%–85%) (Green et al., 2019; Osepchuk, 2002). Besides, there are numerous works in this regard related to the cooling and air conditioning systems (Alqahtani et al., 2023; Hussain et al., 2022; Zawawi et al., 2022).

There are different studies in the literature on the application of microwave technology to the decomposition of different types of wastes such as plastic, tires, and so forth

There are different studies in the literature on the application of microwave technology to the decomposition of different types of wastes such as plastic, tires, and so forth. Mawioo et al. (2017) employed microwave technology for sludge sanitization and drying. They developed a pilot-scale prototype as a reactor for sludge treatment examining different types of sludges, that is, centrifuged waste-activated sludge (C-WAS), non-centrifuged waste-activated sludge (WAS), fecal sludge (FS), and septic tank sludge (SS). They measured the temperature changes, bacteria inactivation and sludge weight/volume reduction during the sludge treatment. They showed successful treatment of sludges using a microwave reactor by achieving complete bacterial inactivation and a sludge weight/volume reduction of almost 60%. Al Mamun et al. (2015) studied the pyrolysis of Scrap tires using microwave technology as an efficient and environmental valorization alternative to combustion- incineration of the waste tire. They claimed that microwave technology can dispose the waste tires completely with no pollution and also can produce alternative fuel. After tire decomposition, the following fractions were obtained including Char residue (48 wt.%), pyro-oil (38 wt.%), and a gas fraction (14 wt.%). The derived pyro-oil is a complex mixture of organic compounds containing various aromatics and can be used as an alternative fuel. Bing et al. (2021) studied microwave pyrolysis of waste tires and showed this method as an efficient and energy-saving way to recycle waste tires. It was demonstrated that a microwave pyrolysis is a novel approach for waste tire recycling since the waste tires contain a high amount of metal oxides additives and carbon black, which can quickly absorb microwave radiation and convert it into heat. They claimed that the total decomposition process of tires by microwave is around 20 min. Moreover, microwave power has a certain effect on the gas product composition which is transferred to a condensation heat exchanger to

release heat, condensed, and collected. Thus, the proper design of the condensation heat exchanger has an important role in the performance of microwave pyrolysis. Mohekar (2018) computationally designed and modeled the main microwave reactor which converts microwave (MW) energy into a usable form of heat energy including the combined effects of electromagnetic wave propagation, heat transfer, and fluid flow. They presented a 2D Multiphysics model using COMSOL software that simulates the interaction between microwaves, heat transfer, and fluid flow during the operation of the microwave. Salema et al. (2017) studied micro vape pyrolysis of corn stalk biomass briquettes which resulted in the production of 19.6% bio-oil, 41.1% biochar, and 54.0% gas at the highest levels. There are other studies in the literature showing the wide applications of microwave technology on waste pyrolysis (Cha et al., 2004; Ge et al., 2021; Nukasani et al., 2017).

There are limited studies on the design and performance of condensers in the microwave reduction process of different waste which has a significant role in the output liquid and gases from the reactor

There are limited studies on the design and performance of condensers in the microwave reduction process of different waste which has a significant role in the output liquid and gases from the reactor. The vapor after the microwave reactor is passed to the condenser which is separated into the liquid phase and gas phase after condensation (Vaštýl et al., 2022). For various waste materials, the condensation temperature is different (Cornell & Wieman, 2002). Typical pyrolysis temperature is in the range of 500–700°C while it is different for various materials (Salema et al., 2017). For waste tire decomposition, the temperature of the material after the pyrolysis has been reported between 200 and 600°C while it is between 100 and 150°C for briquettes or less for different materials (Salema et al., 2017). Soni and Salvi (2020) performed a computational fluid dynamic (CFD) simulation on a shell and multiple tubes heat exchanger for condensation of bio-oil vapor from fast pyrolysis of biomass. In the heat exchanger, the water as the cold fluid was passed through the tubes and the bio-oil vapor was passed through the shell. They studied the performance of the heat exchanger using baffle plates inside the shell to increase the residence time and path of travel of the gas and this improved the heat transfer rate between the cold and hot fluids. Wang et al. (2021) performed an experimental study on a 4-staged condenser for the pyrolysis of biomass vapors. They evaluated the inlet temperature of the gas to the condenser on the condenser efficiency. Wang et al. (2020) studied experimentally the simultaneous effects of condensing temperature and residence time during Walnut shell pyrolysis on the separation and enrichment of bio-oil components.

The relationship between condensing temperature and residence time is effective on the output components of the pyrolysis process. Abdullah et al. (2021) investigated the performance of a triple Tube Heat Exchanger as a liquid collecting system on bio-oil Production during pyrolysis. The gas at the inlet of the heat exchanger was set at the temperatures in the range of 150–250°C. Water as the coolant fluid at ambient temperature was used to absorb the heat from the gas. They reported that the heat exchanger can absorb the maximum heat of 35.77 W from the vapor. Salvi et al. (2021) studied the design of a shell-and-tube condenser for bio-oil recovery from fast pyrolysis of wheat straw biomass and then performed experimental studies on the improved design. The heat exchanger studied had split shell and segmental baffles to divide the shell into various zones and condensate collection points. They demonstrated that increasing the gas flow rate beyond 40 L/min resulted in to decrease in the production of bio-oil.

The objective of this study was to investigate the performance and CFD simulation of the existing shell-and-multiple tube condensing heat exchanger on the cooling of the vapor from the microwave reactor

The objective of this study was to investigate the performance and CFD simulation of the existing shell-and-multiple tube condensing heat exchanger on the cooling of the vapor from the microwave reactor. This paper aims to evaluate the cooling performance of the system by performing a sensitivity analysis on the effective parameters of the system to find out the capacity of the cooling tower. In other words, the analysis performed in this study will be then employed to design the cooling system in the real application. The existing microwave system is used for the waste tire reduction process; however, this study focused on the performance study and sensitivity analysis of the heat exchanger for general applications. Different inlet temperatures and flow rates for both the vapor and water as the hot and cold fluids are examined numerically. It should be noted that the heat exchanger studied in this paper has been rarely discussed in the literature. The paper provides guidelines for the better design of condensers for the microwave reduction process.

2 | SYSTEM DESCRIPTION

The microwave system shown in **Exhibit 1** is designed to reprocess waste tires via depolymerization to recover their original materials, that is, oil, carbon, and steel in addition to the generation of a syn gas.

This microwave system was manufactured on a 1/2 scale in the United Kingdom. The gas from the microwave reactor can be used to generate sufficient electricity to power the system making it energy neutral. The system, generally, includes the microwave reactor, conveying system, and condenser. The output of the microwave reactor is transferred into a separation tank to separate liquid, solid, and vapor. The vapor goes to the condenser to be condensed into the liquid. The remaining gas is transferred to the flare stack to be burnt. As mentioned, the reactor can be also utilized for other applications such as plastic waste, electronic waste, and so forth with different condensing temperatures.

Exhibit 2a displays the picture of the condenser which is a shell-and-multiple tube heat exchanger used to cool the syn gas. The cooling tower is responsible to provide the required cooling capacity of the gas. The details of the heat exchanger can be shown in **Exhibit 2b** including the heat exchanger at the inlet and outlet sides. The lower two flanges are used for access to the oil and liquidated gas from the heat exchanger. The diameters of the pipes are also presented in the photos. The pipes are extended across the shell for six rounds, one inlet tube and one outlet tube. In the middle flanges, there are two holes for the sweep pipes with a diameter of 6 in. The diameters for the inlet and outlet pipes are 8 and 4 in., respectively.

The objective of this study is to perform a CFD simulation to establish the potential capability of the existing heat exchanger by developing a sensitivity analysis

The objective of this study is to perform a CFD simulation to establish the potential capability of the existing heat exchanger by developing a sensitivity analysis. The numerical model is described as follows which is performed based on the real condenser:

2.1 | Geometry and boundary conditions of the CFD model

The heat exchanger studied is a shell-and-tube heat exchanger with multiple pipes. The geometry is generated in ANSYS design modeler software shown in **Exhibit 3a**. The boundary conditions are also illustrated in **Exhibit 3b**. The gas (air) as the hot fluid enters the heat exchanger from the top-right corner and then after passing through the pipes and losing heat to the cold fluid, exits the heat exchanger from the bottom-right corner. The cold fluid (water) enters the shell from the bottom and exits the shell from the top. The walls of the shell are considered insulated to only study the heat exchanger design without considering the ambient effect.

Different temperatures and velocities are considered for the hot and cold fluids to study the performance of the heat exchanger

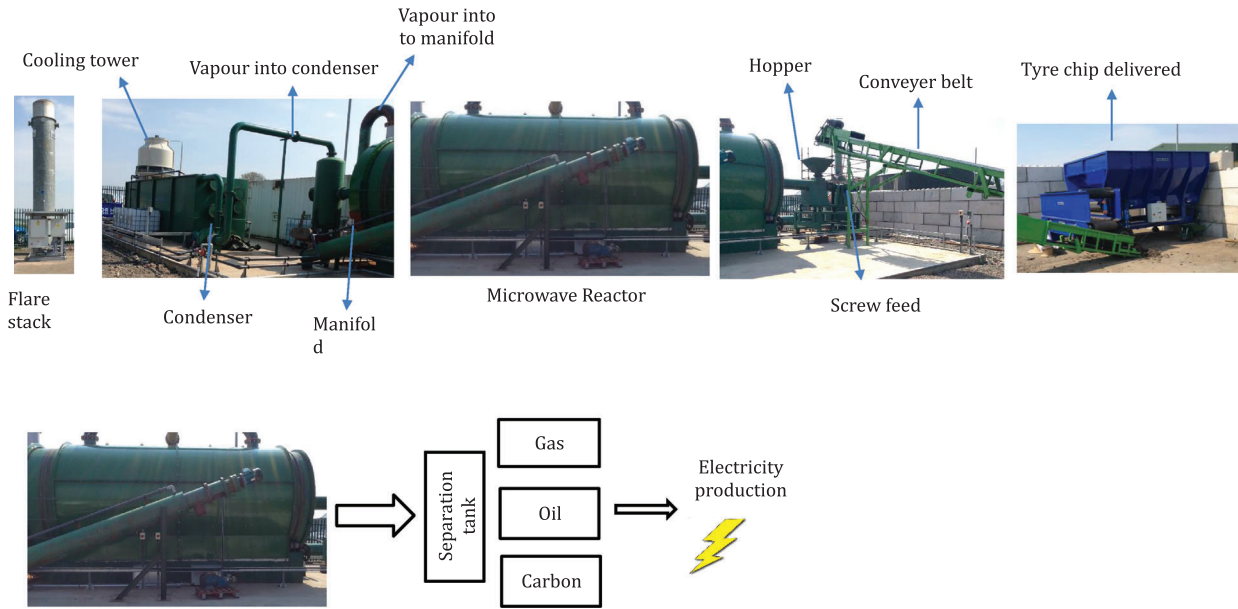


EXHIBIT 1 Microwave system for waste tire pyrolysis. [Color figure can be viewed at wileyonlinelibrary.com]

comprehensively. **Exhibit 4** shows the values of parameters considered in this study.

3 | MATHEMATICAL MODELING

The Reynolds Averaged Navier-Stokes (RANS) is employed to model the turbulent flow by averaging the Navier-Stokes equations and can be expressed as (Speziale, 1998):

$$\rho \bar{u}_k \frac{\partial \bar{u}_i}{\partial x_k} = -\frac{\partial P}{\partial x_i} + \frac{\partial}{\partial x_j} \left(\mu \frac{\partial \bar{u}_i}{\partial x_j} \right) + \frac{\partial R_{ij}}{\partial x_j} \quad (1)$$

where R_{ij} is the Reynolds stress tensor written as:

$$R_{ij} = -\rho \overline{u'_i u'_j} = \mu_t \left(\frac{\partial \bar{u}_i}{\partial x_j} + \frac{\partial \bar{u}_j}{\partial x_i} \right) - \frac{2}{3} \mu_t \frac{\partial \bar{u}_k}{\partial x_k} \delta_{ij} - \frac{2}{3} \rho k \delta_{ij} \quad (2)$$

where μ_t is the turbulent viscosity and k is the turbulent kinetic energy. u'_i and u'_j are turbulent fluctuations considering the starting point of the derivation of the RANS equations as follows:

$$u_i = \bar{u}_i + u'_i \quad (3)$$

The shear-stress transport (SST) k - ω model is used in this study to solve the turbulent flow equation developed by Mentor (Menter, 1994). This model is formed by converting the k - ϵ model into the k - ω formulation to accurately simulate the near-wall region and the free-stream independence of the k - ϵ model in the zones which are far away from the walls (Alamshahi et al., 2020). In this model, the turbulence kinetic energy, k , and the specific dissipation rate, ω , are obtained from the following transport equations for the steady-state condition (Lakshminpathy & Girimaji, 2006):

$$\frac{\partial}{\partial x_i} (\rho k u_i) = \frac{\partial}{\partial x_j} \left(\Gamma_k \frac{\partial k}{\partial x_j} \right) + \tilde{G}_k - Y_k \quad (4)$$

$$\frac{\partial}{\partial x_i} (\rho \omega u_i) = \frac{\partial}{\partial x_j} \left(\Gamma_\omega \frac{\partial \omega}{\partial x_j} \right) + G_\omega - Y_\omega + D_\omega \quad (5)$$

Γ_k and Γ_ω are the effective diffusivities of k and ω obtained as (Wilcox, 2008):

$$\Gamma_k = \mu + \frac{\mu_t}{\sigma_k} \quad (6)$$

$$\Gamma_\omega = \mu + \frac{\mu_t}{\sigma_\omega} \quad (7)$$

\tilde{G}_k and \tilde{G}_ω as representative of turbulence kinetic energy are calculated as:

$$\tilde{G}_k = \min(G_k, 10\rho\beta^*k\omega) \quad (8)$$

$$G_k = -\rho \overline{u'_i u'_j} \frac{\partial u_j}{\partial x_i} \quad (9)$$

and G_ω as representative of the production of ω is:

$$G_\omega = \frac{\alpha}{\nu_t} G_k \quad (10)$$

The turbulent flow equations are solved along with the continuity and energy equations as follows to determine the velocity and temperature distribution in the domain:

$$\nabla \cdot \rho \vec{V} = 0 \quad (11)$$

$$\nabla \cdot (\rho C_p \vec{V} T) = \nabla \cdot (k \nabla T) \quad (12)$$

where C_p and k are the specific heat coefficient and thermal conductivity of the fluid, respectively.



EXHIBIT 2 The photo of (a) the condenser with a cooling tower and (b) components of the condenser with details. [Color figure can be viewed at [wileyonlinelibrary.com](https://onlinelibrary.wiley.com/terms-and-conditions)]

4 | NUMERICAL PROCEDURE

ANSYS FLUENT software is used to perform the CFD simulation and performance evaluation based on a real-scale prototype. SIMPLE scheme is used for the pressure velocity coupling considering the second-order of the pressure and second-order upwind for the

momentum and energy discretization. The value of 10^{-4} is also considered as the convergence criteria.

To find the mesh independent from the number of nodes, two different meshes with the node number of 1,332,480 and 3,826,280 are evaluated and the outlet temperature of the air is considered as the convergence criteria. The inlet temperatures of the air and water are

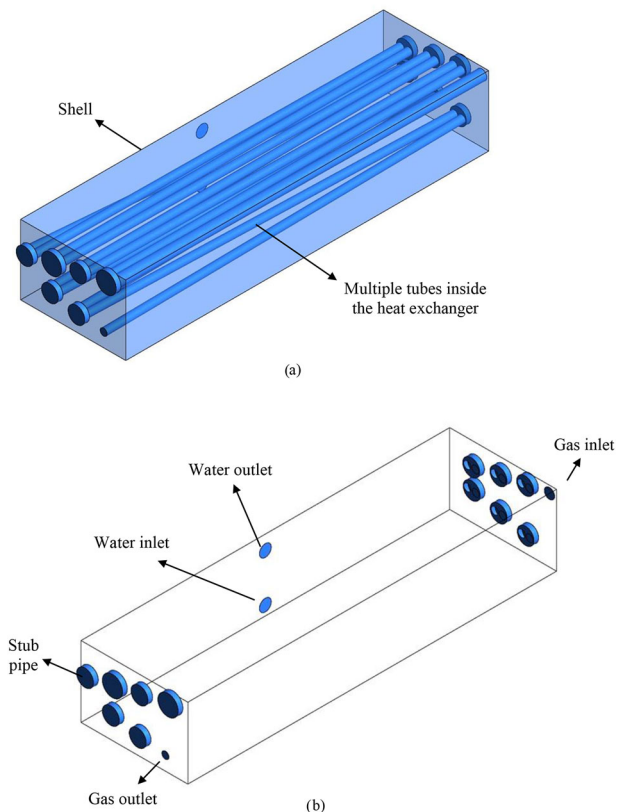


EXHIBIT 3 The schematic of the heat exchanger (a) computational domain and (b) Boundary conditions. [Color figure can be viewed at wileyonlinelibrary.com]

EXHIBIT 4 The values of inlet temperatures and velocities of the hot and cold fluids

	Inlet temperature (°C)	velocity (m/s)
Hot fluid	80, 90, 100	0.25, 0.5, 1
Cold fluid	15, 20, and 25	0.05, 0.1, and 0.15

considered equal to 100 and 20°C, respectively. The inlet velocities of the air and water are considered 0.5 and 0.05 m/s, respectively. The results show negligible changes (less than 2%) in the outlet temperature of the air and thus the mesh with the node number of 1,332,480 is selected for further evaluation. The outlet air temperature for the selected mesh number is 22.29°C.

Due to lack of the experimental data, it is not possible to compare the CFD results with the experimental data. Also, there hasn't been any similar geometry studied in the literature showing the novelty of this study. Thus, to validate the CFD code, a conventional shell-and-tube heat exchanger using a serpentine tube for the cold fluid investigated by Michael et al. (2017) is modeled considering similar dimensions and boundary conditions. The geometry with a serpentine tube is almost similar to the one studied in this paper with three passes. Michael et al. studied a shell-and-tube heat exchanger with a serpentine tube for the cold fluid using water in both shell and tube using ANSYS FLUENT software. The inlet temperatures of the cold and hot water are 300 and

EXHIBIT 5 The values of outlet temperatures of the hot and cold fluids achieved in this study compared with Michael et al. (2017)

	Present study	Michael et al.
Hot fluid	337.5 K	339.3 K
Cold fluid	328.3 K	326.8 K

365 K, respectively. The dimensions and other boundary conditions can be found in Ref. (Michael et al., 2017). Exhibit 5 shows the outlet temperature of the cold and hot fluids achieved in this study compared with Michael et al. (2017). As shown, the results are in good agreement showing the accuracy of the CFD model in this study.

5 | RESULTS AND DISCUSSION

The proposed heat exchanger includes a container (shell) having two holes for the inlet (at the bottom) and an outlet (at the top) for the heat transfer fluid (HTF) (water). In various cases, the water as the cold fluid enters the heat exchanger with different temperatures of 15, 20, and 25°C and velocities of 0.05, 0.1, and 0.15 m/s. For the gas inside the pipes as the hot fluid, different temperatures of 80, 90, and 100°C and velocities of 0.25, 0.5, and 1 m/s are examined. As previously shown in the system description in Exhibit 3, the pipes extend across the shell for six rounds to enhance the heat transfer rate between the hot and cold fluids inside the heat exchanger. As a result of the relatively high temperature of the gas, the heat exchanges with the water (cold fluid) causing an increase in the water temperature at the outlet and thus dropping the gas temperature. It should be noted that the heat exchanger can be used as a condenser in high-temperature microwave applications used for the condensing process of the gas through the pipes. It is worth mentioning that the diameter of the pipe at the inlet section is greater than the outlet section (the pipe diameter reduces through each round across the shell) since the vapor state runs a larger area, and during the condensing process, the vapor changes to liquid, which needs less area to flow.

5.1 | Effect of inlet velocity of the air

Exhibit 6 shows the temperature distribution for the gas pipes with the gas inlet temperature of 100°C and different gas inlet velocities of 0.5 and 1 m/s. The temperature of the tube at the inlet section shows higher values, which change to lower values in each round as the tube is colder due to the heat-exchanging process. The external layer of the gas shows cold temperature due to the flow of the cold HTF around the external side of the tube. The temperature of the external layer of the gas is around 15°C at the outlet section of the system. By increasing the air inlet velocity, the heat exchange process reduces as the gas remains in the tube for a shorter time and in other words, the gas residence time inside the heat exchanger reduces. Thus, less heat transfer from the gas to the HTF occurs, causing a relatively warmer

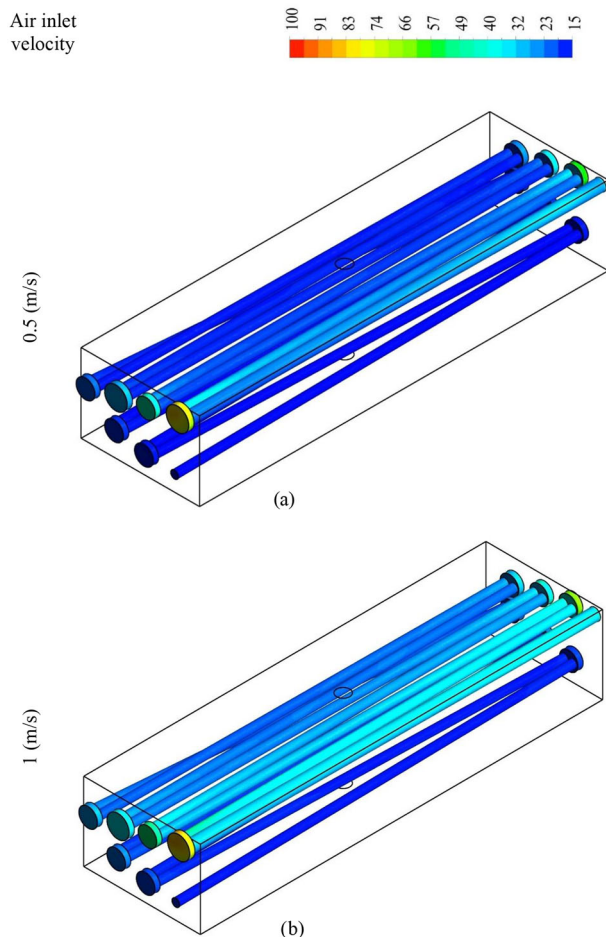


EXHIBIT 6 Temperature distribution of the air inside for different air inlet velocities. [Color figure can be viewed at wileyonlinelibrary.com]

temperature of the external layer of the gas. This behavior indicates that with a faster flow of the gas, a higher output temperature of the gas can be achieved.

Exhibit 7 shows the temperature distribution at the mid-plane of the shell for different air inlet velocities. **Exhibit 7a** illustrates the thermal profiles for the air inlet velocity of 0.5 m/s and **Exhibit 7b** shows the temperature profile for the air inlet velocity of 1 m/s. As mentioned previously, for the slower flow of the air, the air is placed in the tube for a longer time and gained the opportunity to lose more heat to the cold HTF. The cross-section of the first tube (on the top-right) shows an average temperature of 84°C since the air loses some heat when it passes halfway through the shell length. The air shows a colder temperature at the bottom part of the cross-section. The air becomes colder, generally by passing through each tube and reaching thermal equilibrium within the last two tubes before exiting the heat exchanger. The faster flow of the air (**Exhibit 7b**) shows a higher temperature of the air inside the tubes. For the air inlet velocity of 1 m/s, the average temperature for the air at the mid-length of the first tube is 87°C which reduces with passing each tube due to losing more heat. The air temperature reaches thermal equilibrium within the last tube (exit tube).

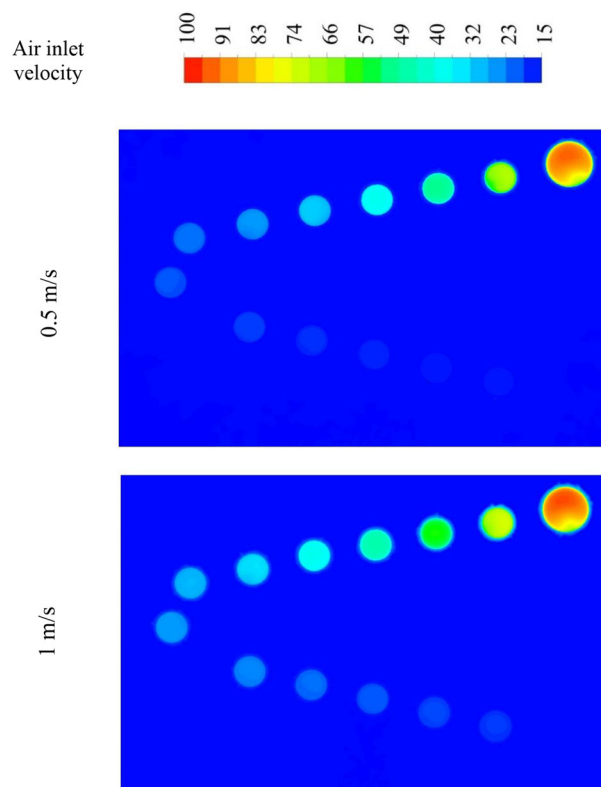


EXHIBIT 7 Temperature distribution at the mid-plane for different air inlet velocities. [Color figure can be viewed at wileyonlinelibrary.com]

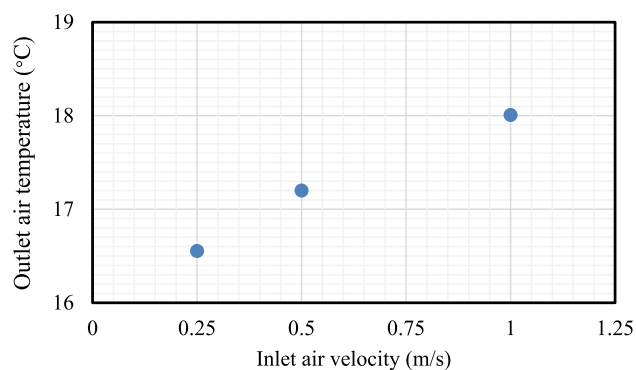


EXHIBIT 8 The variation of air temperature at the outlet for different air inlet velocities. [Color figure can be viewed at wileyonlinelibrary.com]

Exhibit 8 shows the mean outlet air temperature for different inlet velocities of the air. As stated, the higher velocity of the air offers a shorter residence time for the gas inside the tubes and thus fewer heat transfers to the cold HTF. Consequently, a higher temperature is achieved at the air outlet. For slower air flow (0.25 m/s), the outlet temperature of the air reaches 16.5°C; however, for the faster flow (1 m/s), the temperature of the outlet cross-section reaches 18°C.

Exhibit 9 illustrates the heat transfer rate from the air (hot fluid) to the water (cold fluid) for different inlet air velocities. The heat transfer

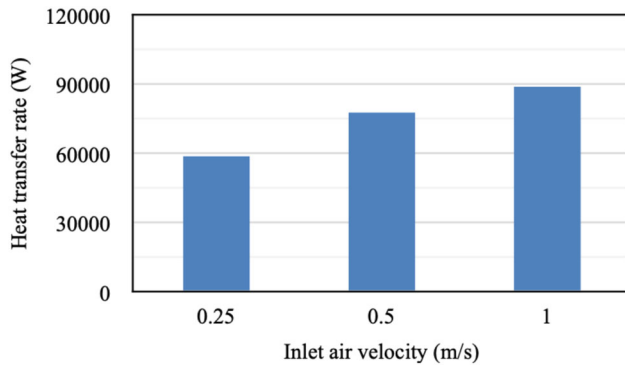


EXHIBIT 9 The variation of heat transfer rate between the hot and cold fluids for different air inlet velocities. [Color figure can be viewed at wileyonlinelibrary.com]

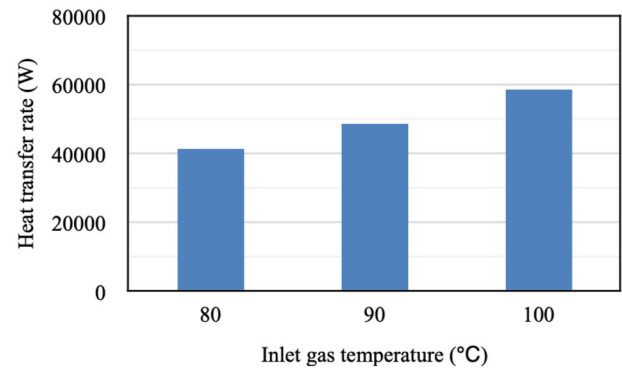


EXHIBIT 11 The variation of heat transfer rate between the hot and cold fluids for different air inlet velocities. [Color figure can be viewed at wileyonlinelibrary.com]

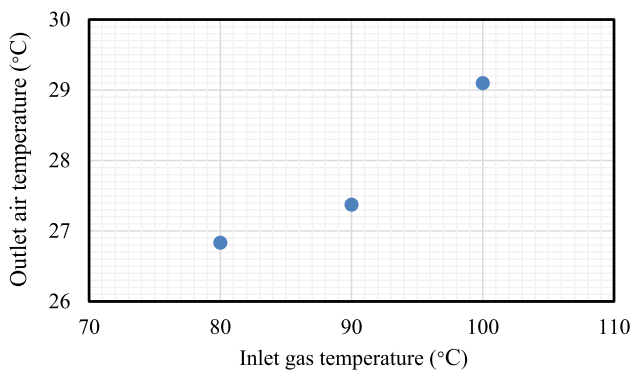


EXHIBIT 10 The variation of air temperature at the outlet for different air inlet temperatures [Color figure can be viewed at wileyonlinelibrary.com]

rate is directly proportional to the inlet air velocity. The heat transfer rate is 58 kW for the inlet air velocity of 0.25 m/s and increases by 32% and 55% when the air velocity rises to 0.5 and 1 m/s, respectively.

5.2 | Effect of inlet temperature of the air

The flow rates and the temperature of the fluid inside the heat exchanger have a great influence on the system's performance. **Exhibit 10** shows the variation of the outlet air temperature as a function of the inlet temperature of the air for different inlet air temperatures of 80, 90, and 100°C. Increasing the inlet air temperature increases the temperature at the outlet; however, the rate of increase from 80 to 90°C is lower than that when the inlet air temperature increases from 90 to 100°C. For the 80°C of inlet air temperature, the outlet temperature is 26.8°C. By increasing the inlet air temperature to 90 and 100°C, the temperature at the outlet section increases by 2.2% and 8.6%, respectively.

The heat transfer rate is also affected by the inlet air temperature. **Exhibit 11** shows the variation of the heat transfer rate for different inlet temperatures of the air. For the air inlet temperature of 80°C,

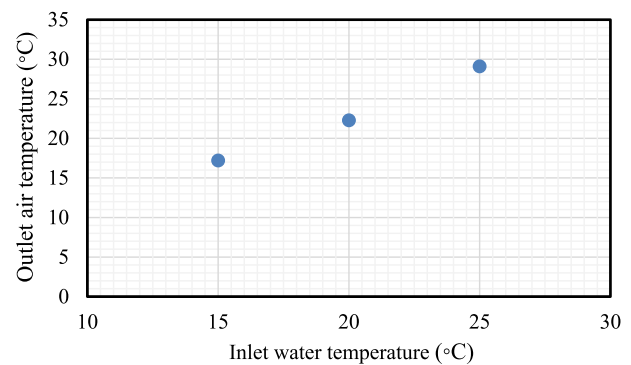


EXHIBIT 12 The variation of air temperature at the outlet for different inlet water temperatures. [Color figure can be viewed at wileyonlinelibrary.com]

the heat transfer rate is 41.3 kW which increases by 17.4% and 42.6% when the inlet air temperature rises to 90 and 100°C, respectively.

5.3 | Effect of inlet temperature of the water

The thermal convection of the HTF has a great impact on the system's performance. **Exhibit 12** illustrates the outlet air temperature as a function of the inlet water temperature for different temperatures of 15, 20, and 25°C. The figure shows that the outlet air temperature is almost directly proportional to the inlet water temperature. The colder HTF can absorb more heat from the air pipe because of the higher temperature difference between the water and the air, which helps more heat transfer through the convection process. The outlet air temperature is equal to 17.2, 22.3, and 29.5°C when the inlet water temperature is 15, 20, and 25°C, respectively.

Through the convection heat transfer, more heat delivers from the air to the cold water, due to the relatively higher temperature difference between them (shown in **Exhibit 13**). A total 77.5 kW of the heat transfer rate delivers when the inlet water temperature is 15°C, whereas this value reduces to 63 and 59 kW when the inlet water temperature is 20 and 25°C, respectively.

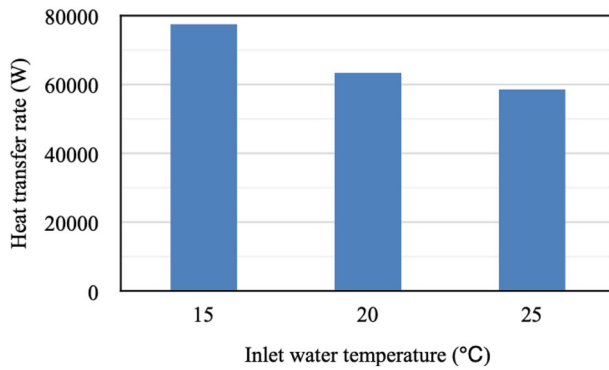


EXHIBIT 13 The variation of heat transfer rate between the hot and cold fluids for different inlet water temperatures. [Color figure can be viewed at wileyonlinelibrary.com]

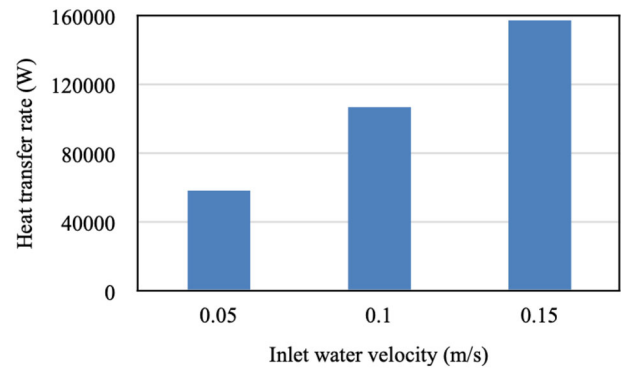


EXHIBIT 15 The variation of heat transfer rate between the hot and cold fluids for different water inlet velocities. [Color figure can be viewed at wileyonlinelibrary.com]

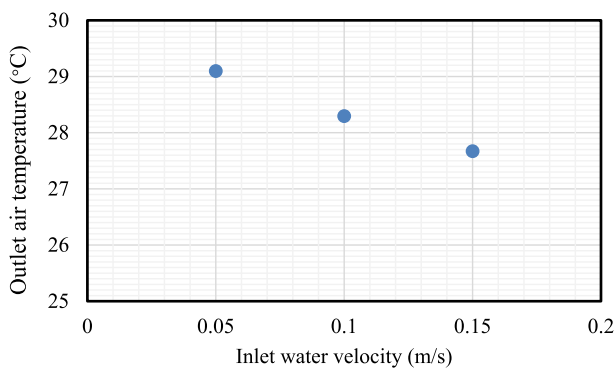


EXHIBIT 14 The variation of air temperature at the outlet for different water inlet velocities. [Color figure can be viewed at wileyonlinelibrary.com]

5.4 | Effect of inlet velocity of the water

By increasing the water velocity at the inlet, continuous cold fresh water is always in the shell, which means that a higher temperature difference between the water and the gas can be provided and consequently, the outlet air temperature drops by increasing the inlet water velocity. **Exhibit 14** displays the variation of air outlet temperature for different inlet water velocities of 0.05, 0.1, and 0.15 m/s. As shown, by increasing the water velocity at the inlet, a higher outlet temperature is achieved for the air. The air temperature at the outlet is around 29°C for the inlet water velocity of 0.05 m/s while it reduces to 28.3 and 27.7°C, respectively, for the inlet water velocities of 0.1 and 0.15 m/s.

Exhibit 15 illustrates the heat transfer rate based on the inlet water velocity. The figure shows that the heat transfer rate is almost proportional to the inlet water velocity directly. The reason is that the fast water flow on the external surface over the pipe extracts more heat from the pipe through the conversion process. Besides, increasing the flow velocity increases the temperature difference between the water in the shell and the air in the tube due to a continuous supply of fresh water. The heat transfer rate is 59 kW when the water inlet tempera-

ture is 0.05 m/s which increases by 80% and 168% when the flow rate increases to 0.1 and 0.15 m/s, respectively.

6 | CONCLUSION

In this study, a CFD analysis was performed to study the performance of a condensation heat exchanger used in the microwave reduction process. The heat exchanger was modeled numerically based on a real condenser used for the waste tires reduction process which is a shell-and-multiple tubes heat exchanger. The output gas from the microwave reactor passes through the tubes of the condenser while cold water from a cooling tower flows inside the shell. A sensitivity analysis was performed to determine the effects of inlet temperatures and mass flow rates of the gas and water. The following are achieved through this study:

- Increasing the inlet air temperature of the gas from 80°C to 90 and 100°C, the temperature at the outlet section increases by 2.2% and 8.6%, respectively when the water inlet temperature is 25°C. The heat transfer rate increases by 17.4% and 42.6% when the inlet air temperature rises from 18°C to 90 and 100°C, respectively.
- The heat transfer rate increases by 32% and 55% when the air velocity rises from 0.25 m/s to 0.5 and 1 m/s, respectively, for the inlet gas and water temperatures of 80 and 15°C, respectively. The outlet temperature of the gas is 16.5°C for the gas inlet velocity of 0.25 m/s while it is 18°C for the gas inlet velocity of 1 m/s.
- The outlet air temperature is equal to 17.2, 22.3, and 29.5°C when the inlet water temperature is 15, 20, and 25°C, respectively. The heat transfer rate is 77.5 kW when the inlet water temperature is 15°C, while it reduces to 63 and 59 kW when the inlet water temperature is 20 and 25°C, respectively.
- The outlet gas temperature is around 29°C for the inlet water velocity of 0.05 m/s while it reduces to 28.3 and 27.7°C, respectively, for the inlet water velocities of 0.1 and 0.15 m/s.

DATA AVAILABILITY STATEMENT

The data that support the findings of this study are openly available in BURA at <https://bura.brunel.ac.uk/>.

ORCID

Salman Masoudi Soltani  <https://orcid.org/0000-0002-5983-0397>

REFERENCES

- Abdullah, N. A., Arif, Z., Suheri, N., & Umar, H. (2021). The influence of triple tube heat exchanger as a liquid collecting system on bio-oil production by pyrolysis process. In Akhyar (Ed.), *Proceedings of the 2nd International Conference on Experimental and Computational Mechanics in Engineering: ICECME 2020, Banda Aceh, October 13–14* (pp. 381–388). Springer Singapore.
- Al Mamun, A., Salam, B., Farid Nasir Ani, F., Md, S. k., & Kabir, S. M. H. (2015). *Pyrolysis of scrap tyre by microwave* (Working Paper).
- Alamshahi, F., Rahimzadeh, H., Rafee, R., Moghimi, M. A., & Talebizadehsardari, P. (2020). Effects of roughness on the performance of a threaded zigzag demister using RSM and $k-\omega$ turbulent models. *Sādhanā*, 45(1), 283. <https://doi.org/10.1007/s12046-020-01510-2>
- Alqahtani, S., Ali, H. M., Farukh, F., & Kandan, K. (2023). Experimental and computational analysis of polymeric lattice structure for efficient building materials. *Applied Thermal Engineering*, 218, 119366. <https://doi.org/10.1016/j.applthermaleng.2022.119366>
- Bing, W., Hongbin, Z., Zeng, D., Yuefeng, F., Yu, Q., & Rui, X. (2021). Microwave fast pyrolysis of waste tires: Effect of microwave power on product composition and quality. *Journal of Analytical and Applied Pyrolysis*, 155, 104979. <https://doi.org/10.1016/j.jaap.2020.104979>
- Budarin, V. L., Shuttleworth, P. S., Farmer, T. J., Gronnow, M. J., Pfaltzgraff, L., Macquarrie, D. J., & Clark, J. H. (2015). The potential of microwave technology for the recovery, synthesis and manufacturing of chemicals from bio-wastes. *Catalysis Today*, 239, 80–89. <https://doi.org/10.1016/j.cattod.2013.11.058>
- Cha, C., Wallace, S., George, A., & Rogers, S. (2004). Microwave technology for treatment of fume hood exhaust. *Journal of Environmental Engineering-ASCE*, 130, 338–348. [https://doi.org/10.1061/\(ASCE\)0733-9372\(2004\)130:3\(338\)](https://doi.org/10.1061/(ASCE)0733-9372(2004)130:3(338))
- Cornell, E. A., & Wieman, C. E. (2002). Nobel Lecture: Bose-Einstein condensation in a dilute gas, the first 70 years and some recent experiments. *Reviews of Modern Physics*, 74(3), 875–893. <https://doi.org/10.1103/RevModPhys.74.875>
- Das, S., Mukhopadhyay, A. K., Datta, S., & Basu, D. (2009). Prospects of microwave processing: An overview. *Bulletin of Materials Science*, 32(1), 1–13.
- Ge, S., Yek, P. N. Y., Cheng, Y. W., Xia, C., Mahari, W. A. W., Liew, R. K., Liew, R. K., Peng, W., Yuan, T.-Q., Tabatabaei, M., Aghbashlo, M., Sonne, C., & Lam, S. S. (2021). Progress in microwave pyrolysis conversion of agricultural waste to value-added biofuels: a batch to continuous approach. *Renewable and Sustainable Energy Reviews*, 135, 110148.
- Green, M., Van Tran, A. T., Smedley, R., Roach, A., Murowchick, J., & Chen, X. (2019). Microwave absorption of magnesium/hydrogen-treated titanium dioxide nanoparticles. *Nano Materials Science*, 1(1), 48–59. <https://doi.org/10.1016/j.nanoms.2019.02.001>
- Hussain, I., Bibi, F., Bhat, S. A., Sajjad, U., Sultan, M., Ali, H. M., Azam, M. W., Kaushal, S. K., Hussain, S., & Yan, W.-M. (2022). Evaluating the parameters affecting the direct and indirect evaporative cooling systems. *Engineering Analysis with Boundary Elements*, 145, 211–223. <https://doi.org/10.1016/j.enganabound.2022.09.016>
- Lakshminpathy, S., & Girimaji, S. (2006). Partially-averaged Navier-Stokes method for turbulent flows: kw model implementation. Paper presented at the 44th AIAA aerospace sciences meeting and exhibit.
- Lam, S. S., & Chase, H. A. (2012). A review on waste to energy processes using microwave pyrolysis. *Energies*, 5(10), 4209–4232. <https://doi.org/10.3390/en5104209>
- Lawag, R. A., & Ali, H. M. (2022). Phase change materials for thermal management and energy storage: A review. *Journal of Energy Storage*, 55, 105602. <https://doi.org/10.1016/j.est.2022.105602>
- Liu, M., Yin, X., Guo, X., Hu, L., Yuan, H., Wang, G., Wang, F., Chen, L., Zhang, L., & Yu, F. (2019). High efficient oxygen reduction performance of Fe/Fe₃C nanoparticles in situ encapsulated in nitrogen-doped carbon via a novel microwave-assisted carbon bath method. *Nano Materials Science*, 1(2), 131–136. <https://doi.org/10.1016/j.nanoms.2019.04.003>
- Ludlow-Palafox, C., & Chase, H. A. (2001). Microwave-induced pyrolysis of plastic wastes. *Industrial & Engineering Chemistry Research*, 40(22), 4749–4756.
- Mawioo, P. M., Garcia, H. A., Hooijmans, C. M., Velkushanova, K., Simonić, M., Mijatović, I., & Brdjanovic, D. (2017). A pilot-scale microwave technology for sludge sanitization and drying. *Science of the Total Environment*, 601, 1437–1448. <https://doi.org/10.1016/j.scitotenv.2017.06.004>
- Menter, F. R. (1994). Two-equation eddy-viscosity turbulence models for engineering applications. *AIAA Journal*, 32(8), 1598–1605. <https://doi.org/10.2514/3.12149>
- Metaxas, A. (1991). Microwave heating. *Power Engineering Journal*, 5(5), 237–247. <https://doi.org/10.1049/pe:19910047>
- Michael, S., John, K. K., Krishnan, A., Shanid, K., & Mathew, M. (2017). Comparative CFD analysis of shell and serpentine tube heat exchanger. *International Research Journal of Engineering and Technology*, 4, 1171–1175.
- Mohekar, A. A. (2018). Computational modeling of triple layered microwave heat exchanger [MS Thesis].
- Motasemi, F., & Afzal, M. T. (2013). A review on the microwave-assisted pyrolysis technique. *Renewable and Sustainable Energy Reviews*, 28, 317–330. <https://doi.org/10.1016/j.rser.2013.08.008>
- Nukasani, S., Prince, M., & Sreeja, R. (2017). Review on microwave assisted extraction technique. *International Journal of Pure and Applied Bioscience*, 5(3), 1065–1074.
- Osepchuk, J. M. (2002). Microwave power applications. *IEEE Transactions on Microwave Theory and Techniques*, 50(3), 975–985. <https://doi.org/10.1109/TMTT.2002.989981>
- Salema, A. A., Afzal, M. T., & Bennamoun, L. (2017). Pyrolysis of corn stalk biomass briquettes in a scaled-up microwave technology. *Bioresource Technology*, 233, 353–362. <https://doi.org/10.1016/j.biortech.2017.02.113>
- Salvi, B. L., Soni, T., Jindal, S., & Panwar, N. L. (2021). Design improvement and experimental study on shell and tube condenser for bio-oil recovery from fast pyrolysis of wheat straw biomass. *SN Applied Sciences*, 3(2), 173. <https://doi.org/10.1007/s42452-021-04165-8>
- Soni, T., & Salvi, B. L. (2020). A computational fluid dynamics study of a condenser for condensation of bio-oil vapour from fast pyrolysis of biomass. *International Journal of Renewable Energy Technology*, 11(4), 335–345. <https://doi.org/10.1504/ijret.2020.113770>
- Speziale, C. G. (1998). Turbulence modeling for time-dependent RANS and VLES: a review. *AIAA Journal*, 36(2), 173–184. <https://doi.org/10.2514/2.7499>
- Thostenson, E., & Chou, T.-W. (1999). Microwave processing: Fundamentals and applications. *Composites Part A: Applied Science and Manufacturing*, 30(9), 1055–1071. [https://doi.org/10.1016/S1359-835X\(99\)00020-2](https://doi.org/10.1016/S1359-835X(99)00020-2)
- Vaštyl, M., Jankovská, Z., Cruz, G. J. F., & Matějová, L. (2022). A case study on microwave pyrolysis of waste tyres and cocoa pod husk; effect on quantity and quality of utilizable products. *Journal of Environmental Chemical Engineering*, 10(1), 106917. <https://doi.org/10.1016/j.jece.2021.106917>
- Wang, C., Luo, Z., Li, S., & Zhu, X. (2020). Coupling effect of condensing temperature and residence time on bio-oil component enrichment during the condensation of biomass pyrolysis vapors. *Fuel*, 274, 117861. <https://doi.org/10.1016/j.fuel.2020.117861>

- Wang, C., Yang, Y., Ma, Y., & Zhu, X. (2021). Experimental study on the composition evolution and selective separation of biomass pyrolysis vapors in the four-staged indirect heat exchangers. *Bioresource Technology*, 332, 125115. <https://doi.org/10.1016/j.biortech.2021.125115>
- Wilcox, D. C. (2008). Formulation of the kw turbulence model revisited. *AIAA Journal*, 46(11), 2823–2838. <https://doi.org/10.2514/1.36541>
- Zawawi, N. N., Azmi, W. H., Ghazali, M. F., & Ali, H. M. (2022). Performance of air-conditioning system with different nanoparticle composition ratio of hybrid nanolubricant. *Micromachines*, 13(11). <https://doi.org/10.3390/mi13111871>
- Zhou, L., Xu, P., & Qin, F. (2022). Enhanced thermal conductivity and microwave dielectric properties by mesostructural design of multiphase nanocomposite. *Nano Materials Science*, 4(2), 133–138. <https://doi.org/10.1016/j.nanoms.2021.08.002>

How to cite this article: Babaei-Mahani, R., Sardari, P. T., Soltani, S. M. *, Mohammed, H. I., Kunczewicz, Z., & Starr, C. (2024). CFD simulation of a shell and multiple tubes condensing heat exchanger in a modified microwave plant applied for reprocessing End of Life Tires (ELTs). *Environmental Quality Management*, 33(4), 19–29. <https://doi.org/10.1002/tqem.21971>